Dual-Band Ferrite Circulators Operating on Weak Field Conditions: Design Methodology and Bandwidths' Improvement

Vincent Olivier, Laure Huitema, *Member, IEEE*, Bertrand Lenoir, Hamza Turki, Christophe Breuil, Philippe Pouliguen, *Member, IEEE* and Thierry Monediere

***Abstract*— This article presents the principle of coupling fundamental and upper eigenmodes of a ferrite cavity for demonstrating a dual-band stripline circulator. The weak field operation is used for increasing circulation bandwidths and choosing the ratio between the two circulation central frequencies. Indeed, an eigenmode study is presented which identifies parameters that influence the working frequencies and the circulation direction, which can be either the same between the first and the second bands (unidirectional circulator) or different (bidirectional circulator). Two prototypes of dual-band circulators (uni- and bidirectional) have been designed and their measurements validate the developed methodology based on modal analyses.**

***Index Terms*— Bidirectional, dual-band, ferrite, modal analysis, unidirectional, upper modes, Y-junction circulators.**

I. Introduction

FERRITE circulators are nonreciprocal devices commonly used in microwaves to connect a transmitter (TX)/receiver (RX) system to a single antenna or to isolate RF sources. The expansion of multiband systems [1] has led to the development of RF functions, such as antennas or filters, that can work simultaneously over several frequency bands. While the literature presents many studies on multiband antennas or filters [2]–[6], only a few articles present multiband circulators [7]–[9]. However, the design of circulators operating in several frequency bands is necessary to design complete multiband systems and maintain insulation while reducing space requirements.

Manuscript received December 5, 2019; revised February 21, 2020; accepted March 19, 2020. Date of publication April 29, 2020; date of current version July 1, 2020. This work was supported in part by ANR (French National Research Agency) in the framework of the collaborative laboratory "INOGYRO," established between the XLIM Research Institute, 87060 Limoges, France, and Inoveos, Brive-la-Gaillarde, France, and in part by French Defense Innovation Agency. *(Corresponding author: Vincent Olivier.)*

Vincent Olivier is with the XLIM Research Institute, in collaboration with Inoveos Company, 19100 Limoges, France (e-mail: vincent.olivier@unilim.fr).

Laure Huitema and Thierry Monediere are with the "Antennas and Signals" Department, XLIM Research Institute, University of Limoges, 87060 Limoges, France (e-mail: laure.huitema@unilim.fr; thierry.monediere@unilim.fr).

Bertrand Lenoir, Hamza Turki, and Christophe Breuil are with Inoveos, 19100 Brive-la-Gaillarde, France (e-mail: b.lenoir@inoveos.com; hturki@inoveos.com; cbreuil@inoveos.com).

Philippe Pouliguen is with French Defense Innovation Agency, 75509 Paris, France.

Color versions of one or more of the figures in this article are available online at http://ieeexplore.ieee.org.

Digital Object Identifier 10.1109/TMTT.2020.2988003

Ferrite circulators have been the subject of many researches for several decades [10]–[15]. Most of the researches are based on the study of reverse polarization eigenmodes in ferrite cavities and their pairing to obtain a circulation function [10], [11], [13]. In most cases, only fundamental modes are excited, leading to a single-band circulation phenomenon [10], [11]. Among these references, two distinct operation ways can be distinguished: the strong and the weak field operations. The main advantage of designing a circulator working in a weak field condition is that wider circulation bandwidths (BWs) can be achieved as long as they can be successfully matched [11], [16]. Indeed, compared with strong field operations, impedance matching is more difficult to obtain and often requires complex central conductors [17]. These two modes of operation have already been widely studied, but only for circulators operating on a single frequency band.

Indeed, only a few studies on dual-band circulators have already been presented in the literature [7]–[9]. Razavipour *et al.* [8] designed a dual-band circulator based on waveguide, while Turki *et al.* [7] developed, realized, and measured a stripline dual-band circulator for the first time. The latter present that the second circulation band is obtained by coupling the upper modes in addition to the fundamental modes usually used. However, this circulator operated with a polarized ferrite in strong field conditions leading to limited BWs and requires the use of bulky magnets. Moreover, the two operating bands are strongly linked and the frequency gap between these two working bands is very difficult to choose.

The main objective of this work is to develop a methodology for designing a circulator working on two preselected frequency bands. Indeed, we will show that working in the weak field area and with a complex central conductor will improve the BW while choosing the two central circulation frequencies.

Section II will present an eigenmode study of the resonance frequencies in a ferrite cavity. The frequency dependence of eigenmodes is studied according to the saturation magnetization, the ferrite disks' radius, and the shape of the central conductor. The purpose of this study is to identify the parameters that affect the frequency ratio between 1) counter-rotating modes to increase the impedance BW and 2) the fundamental and upper modes to show how the frequency gap between the circulation bands can be modified.

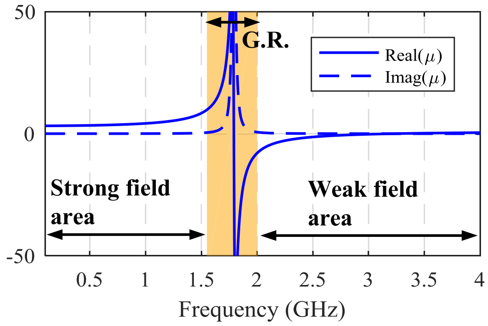

Fig. 1. Curves of μ term of the Polder's permeability tensor as a function of frequency (Hi = 51 kA/m, 4πMs = 1450 G, and $\Delta H = 0.16$ kA/m).

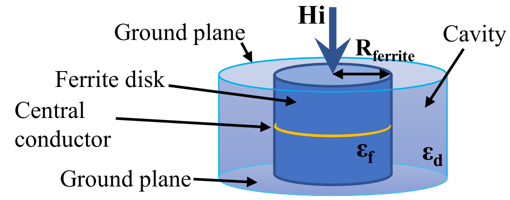

Fig. 2. Ferrite resonator model.

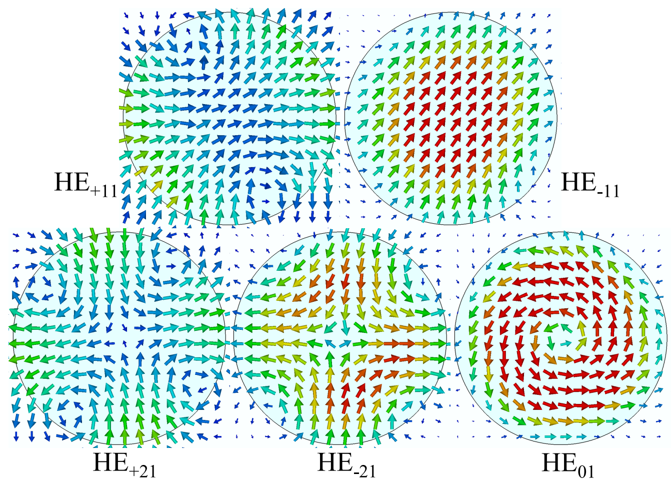

Fig. 3. Stationary pattern issued from the $\mathrm{HE}_{\pm\mathrm{nm}}$ modes.

This section will also highlight that an inversion in the order of appearance of the upper modes can occur when changing the shape of the central conductor. This interesting property will be used to change the circulation direction between the first and the second operating frequencies.

At the end of Section II, two central conductors are chosen for designing, and in Section III, two circulators are chosen for designing: one with unidirectional circulation and the other providing a bidirectional circulation. Indeed, this section will exhibit the coupling of modes within the two circulation frequency bands, simultaneously. The measurement of prototypes will validate the proposed methodology and their performances will be compared with those of the circulators already produced in strong field [7].

II. Modal Analysis

A. Eigenmodes' Resonance Frequencies' Computation

The nonreciprocal properties of passive circulators are obtained using ferrite materials. These materials are ceramics with a high permittivity and permeability tensor models have been defined to characterize their anisotropy [18]–[20]. In this study, only saturated ferrites are used, which allow the Polder's permeability tensor model [19] to be implemented. Fig. 1 shows the frequency dependence of Polder's tensor diagonal term μ and highlights the existence of two distinct areas, separated by the gyromagnetic resonance (GR). The frequency band before the resonance is called the strong field operating area, while the second operating zone, located after the resonance, is the weak field area.

The key element in the development of dual-band circulators is based on an eigenmode analysis because it determines both their working frequencies and the circulation direction.

This eigenmode analysis is based on cavities (Fig. 2) composed of two ferrite disks with a central metallic conductor, which is usually a disk of same diameter as the ferrite disks.

Eigenmode studies of resonant cavities using ferrite materials [7], [13], [21], [22] use either simple models when boundaries are assumed to be perfect magnetic walls or more complex models when considering the real interface between the ferrite resonator and the dielectric medium surrounding it. The latter shows pairs of counter-rotating hybrid modes $\mathrm{HE}_{\pm nm}$ where $(n, m) \in N^2$, close to those obtained in measurement [13]. The integers n and m represent the azimuthal and the radial variations, respectively. A numerical method to determine the eigenmodes' frequencies in the ferrite cavity is presented in [7] and shows a good agreement with analytical and experimental frequencies.

In this article, the numerical method presented in [7] is combined with a MATLAB program to generate charts presenting the frequency dependence of eigenmodes according to ferrite intrinsic parameters. This method starts with the electromagnetic (EM) simulation of a structure, weakly excited with magnetic probes. Then, a mapping of the electric and magnetic fields in the ferrite disks allows the identification of the modes, that is, the (n, m) values.

Fig. 3 shows the first five modes, with the mapping of their H-fields in a cutting plane at half the height of the upper ferrite.

The combination with the MATLAB code allows the sweeping of some parameters (dimensional or intrinsic parameters) and the study of the evolution of eignemodes' resonance frequencies as a function of these parameters. An example presented in Fig. 4 shows the internal dc magnetic field (Hi) sweeping in strong and weak fields for a ferrite circular cavity with a radius of 6.6 mm and a saturation magnetization 4πMs = 1450 G.

These results highlight the differences between strong and weak field operating modes.

1) Counter-rotating modes are closer to each other for the strong field, while they are more distant in weak field, that is, the frequency gap between counter-rotating modes is larger in weak field.
2) The order of appearance is not always the same in weak field, which implies that the upper modes can be interposed between the pair of counter-rotating modes

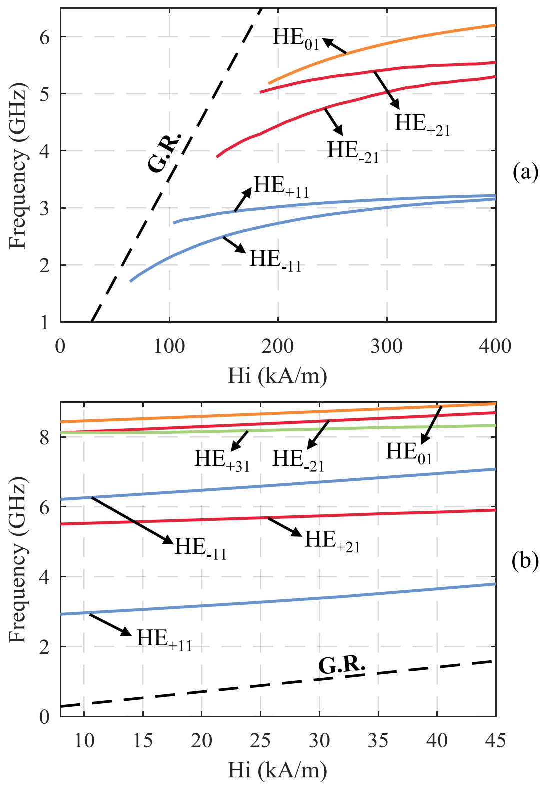

Fig. 4. Eigenmodes' resonance frequencies in a ferrite cavity as a function of the internal static magnetic field (Hi), in (a) strong field and (b) weak field, calculated by a numerical method ($R_{\text{ferrite}} = 6.6$ mm and 4πMs $= 1450$ G).

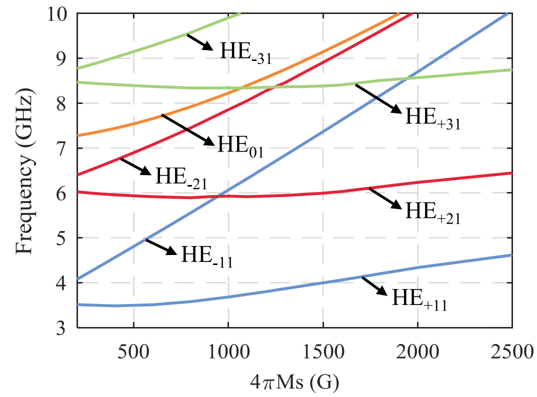

Fig. 5. Computed eigenmodes' resonance frequencies in a ferrite cavity as a function of saturation magnetization (4πMs). Model parameters: $\varepsilon_r = 14$, $R_{\text{ferrite}} = 6.6$ mm, and Hi $= 51$ kA/m.

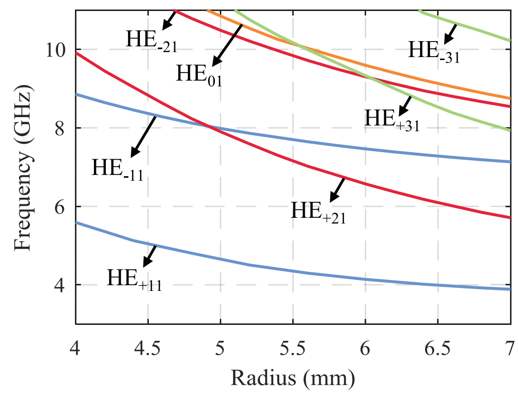

Fig. 6. Computed eigenmodes' resonance frequencies in a ferrite cavity as a function of ferrite disks radius, Model parameters: $\varepsilon_r = 14$, 4πMs $= 1450$ G, and Hi $= 51$ kA/m.

$\text{HE}_{\pm 11}$. Indeed, in Fig. 4(b) the HE_{+21} mode appears before the HE_{-11} mode.

It should be reminded that the objectives of this article are to develop a dual-band circulator with wider BWs than those presented in the literature and with a ratio between the two working frequencies that can be chosen.

Single-band studies presented in [22] have shown that a large frequency gap between counter-rotating modes leads to wider BWs. Therefore, considering all the previous intermediate conclusions, the weak field operation is chosen for this work, and the next paragraph will detail the effect of other parameters on eigenmodes.

B. Parametric Study

Resonance frequencies of eigenmodes are influenced by many parameters, and even if many studies deal with their variations [11], [22], none of them tried to adjust the frequencies of the upper modes $\text{HE}_{\pm 21}$ with those of $\text{HE}_{\pm 11}$.

Thanks to the numerical model described in the previous paragraph (Section II-A), the influence of the ferrite radius, the saturation magnetization, and the shape of the central conductor are discussed.

1) Influence of 4πMs and Ferrite Radius: The curves in Figs. 5 and 6 show the variation in the eigenmodes' resonance frequencies in a ferrite cavity, as a function of the saturation magnetization (4πMs) and the radius of ferrite disks, respectively.

These curves show a first overview of how eigenmodes' resonance frequencies can be modified in ferrite cavities. Indeed, by modifying the saturation magnetization (Fig. 5), the upper modes' configuration can be modified. For example, depending on the saturation magnetization, the HE_{+31} eigenmode can be above the $\text{HE}_{\pm 21}$ modes, interposed between them, or between $\text{HE}_{\pm 11}$.

The eigenmode resonance frequencies also depend on the radius of the cavity (R_{ferrite}). Indeed, it influences both the resonance frequencies' values and the frequency ratio between fundamentals and upper counter-rotating pairs of modes.

It therefore appears that these different parameters can be arranged to obtain two operating bands at predefined frequencies. However, a major disadvantage when using the weak field operation is that the use of a central disk conductor is not always possible if the dielectric surrounding the ferrite disks is air. Indeed, the impedance of the lines presented at the dielectric ferrite interface is too low to be realistic [11]. The most common solution to address this issue is to use different central conductor's shapes, rather than a disk.

2) Influence of Central Conductor Shape: The classical conductor's shapes are based on a WYE configuration [Fig. 7(a)] [23] or a WYE configuration with stubs [Fig. 7(b)] studied in [24].

A first study on the basic WYE shape has been carried out. In this framework, the impact of the width W [Fig. 7(a)] of the WYE line is studied and presented in Fig. 8.

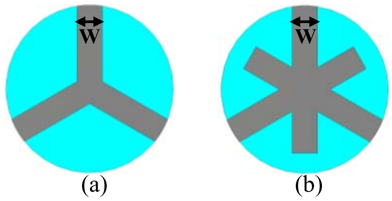

Fig. 7. (a) Central conductor WYE and (b) WYE with stubs.

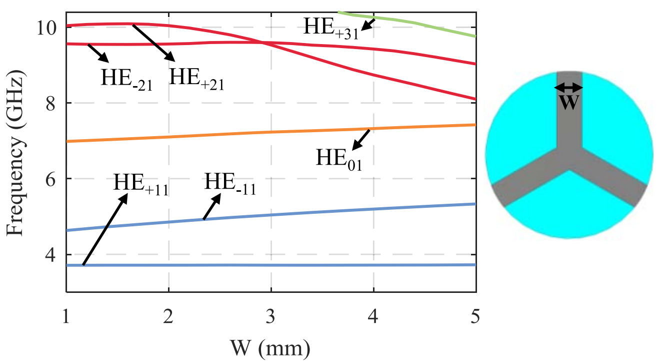

Fig. 8. Computed eigenmodes' resonance frequencies in a ferrite cavity as a function of linewidth (W) [Fig. 7(a)]. Model parameters: $\varepsilon_r = 14$, 4πMs $= 1450$ G, Hi $= 51$ kA/m, and $R_{\text{ferrite}} = 6.6$ mm.

Several conclusions can be extracted from the curves presented in Fig. 8.

1) The width W has a higher influence on the upper modes. Indeed, with low values of W (less than 1.5 mm), the frequency gap between the eigenmodes $\text{HE}_{\pm 11}$ (the central frequency of the HE_{+11} and HE_{-11} modes) and $\text{HE}_{\pm 21}$ is more than 5 GHz, while with higher values of W, the gap between $\text{HE}_{\pm 11}$ and $\text{HE}_{\pm 21}$ frequencies is less than 3 GHz.
2) An inversion of the order of $\text{HE}_{\pm 21}$ modes' appearance occurs when $W = 3$ mm. Indeed, above this width, the HE_{-21} mode appears before the HE_{+21} mode, while for narrower line widths, the HE_{+21} mode appears before HE_{-21}. This order of appearance of these modes is of great importance since Section III will show that it defines the circulation direction, which can be either the same between the first and the second bands (unidirectional circulator) or different (bidirectional circulator).

The WYE topology with stubs presented in Fig. 7(b) is also studied with the sweep of the linewidth W of the central conductor. Fig. 9 shows the frequency dependence of modes with the modification of the width.

With this central conductor, the same phenomena can be found. Indeed, the ratio between the pairs of modes varies and the order in which the upper modes appear depends on the W value. Moreover, new modes appear around the lower frequency band. These modes come from a change in the sign of the effective permeability combined with the presence of stubs. One mode is close to the HE_{+11} mode, while the other one is similar to the HE_{-11} mode. These modes are close to the fundamental ones since their mapping show an azimuthal variation ($n = 1$) and a radial variation ($m = 1$). To simplify the classification, they have been referenced as the HE_{-11} and HE_{+11} modes.

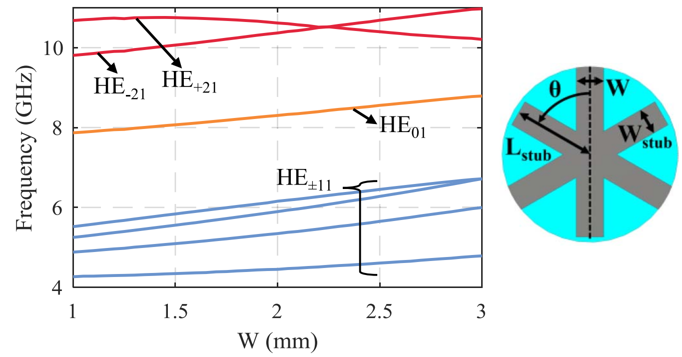

Fig. 9. Computed eigenmodes' resonance frequencies in a ferrite cavity as a function of linewidth (W) [Fig. 7(b)]. Model parameters: $\varepsilon_r = 14$, 4πMs $= 1450$ G, Hi $= 51$ kA/m, $R_{\text{ferrite}} = 6.6$ mm, $\theta = \pi/3$ rad, $L_{\text{stub}} = 6.2$ mm, and $W_{\text{stub}} = W$.

TABLE I
PARAMETERS INFLUENCING EIGENMODES' RESONANCE FREQUENCIES

Parameters	Δf2/f1	Δf+/f-	Upper modes order modification
Increase of *4πMs*	↘	↗↗	No
Increase of *Hi* (Weak field)	↗	↗	No
Increase of Radius	↘	↘	No
Increase of *W* (WYE with stubs)	↗	↗	Yes

This modal study based on a numerical method showed that several parameters can be adjusted to change the frequencies of eigenmodes. Table I summarizes the results of these modal studies. The evolution of the ratio between the pairs of modes $\text{HE}_{\pm 11}$ and $\text{HE}_{\pm 21}$ is presented with the $\Delta f2/f1$ column. The parameter $\Delta f{+}/f{-}$ indicates the frequency gap variation between the positive and negative counter-rotating modes. The last column corresponds to the opportunity to change the order in which the upper modes appear.

Table I identifies which parameters need to be changed according to the expected eigenmodes' frequencies, which are directly linked to the circulator working frequencies. Indeed, the operation of the circulator and its performances will be governed by these modes. This will be discussed in the next paragraph, which will link the eigenmode analysis to the EM study.

C. Eigenmode Analysis and Configuration of the Final Resonator

The eigenmode analysis is linked to the circulation, and therefore changing the frequency of modes and their order will influence the circulation phenomenon. The parameters influencing the resonance frequencies of the eigenmodes have been identified.

To understand the influence of the appearance order of the modes on the EM parameters, the modal results presented in Fig. 9 are used since they show a clear inversion of the HE_{-21} and HE_{+21} modes (when $W = 2.2$ mm).

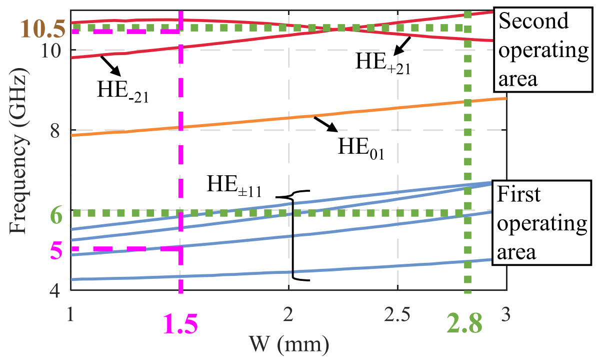

Fig. 10. Computed eigenmodes' resonances frequencies in a ferrite cavity as a function of linewidth (W) [Fig. 7(b)]. Model parameters: $\varepsilon_r = 14$, 4πMs = 1450 G, Hi = 51 kA/m, and $R_{\text{ferrite}} = 6.6$ mm.

Therefore, a WYE with stubs' configuration for the central conductor is chosen to develop two circulators with different linewidth values, that is, $W = 1.5$ mm and $W = 2.8$ mm. The ferrite disks of both resonators are identical, as well as their internal dc magnetic field.

Fig. 10 shows the results of Fig. 9 and points out the two line widths W previously identified. The circulation phenomenon occurs when the pairs of modes are excited. Therefore, for a dual-band circulator, both the $\text{HE}_{\pm 11}$ and $\text{HE}_{\pm 21}$ pairs need to be excited. If excited, the circulation frequency takes place near the middle of each pair.

From Fig. 10, the expected circulation frequencies for $W = 1.5$ mm are around 5 and 10.5 GHz, while they are about 6 and 10.5 GHz for $W = 2.8$ mm. Moreover, the order of appearance of the upper modes $\text{HE}_{\pm 21}$ is inverted when comparing the two cases, which will result in the inversion of the circulation direction.

These two resonators lead to the design of two circulators with different operating conditions (uni- and bidirectional) presented in Section III.

III. Dual-Band Circulator Design

In this section, ferrite resonators and central conductors previously defined are used to design two different circulators. The material used for ferrite disks is a Y215 type which has a saturation magnetization of 1450 G, the internal dc magnetic field within the ferrite is 51 kA/m, and the relative permittivity is 14. It should be noted that the manufacturer gives this relative permittivity of 14 with an accuracy of ±5%. The first circulator will have a unidirectional operation with circulation phenomena around 5 and 10.5 GHz. The second circulator will have a bidirectional operation, that is, with the two circulation phenomena will occur in the opposite directions around 6 and 10.5 GHz.

A. Unidirectional Dual-Band Circulator

This first circulator has a central conductor WYE with stubs defined in Fig. 7(b) with line widths of 1.5 mm. Using the previous methodology on the uncoupled resonators, the eigenmodes' frequencies are computed. The results presented in Fig. 11 show that each $|S_{11}|$ peak corresponds to the eigenmodes presented in Fig. 10.

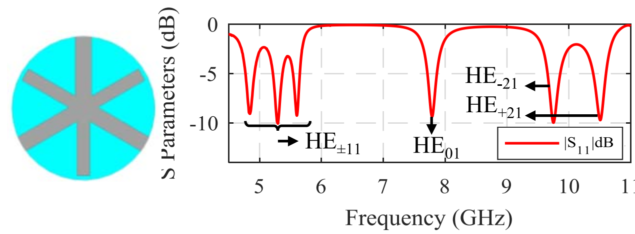

Fig. 11. Central conductor WYE with stubs with $W = 1.5$ mm and EM simulations of uncoupled ferrite resonator.

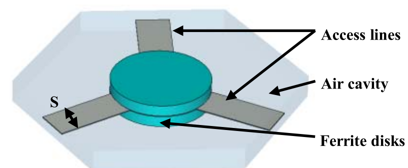

Fig. 12. Simplifies numerical model for outer lines' sizing.

As shown previously, the fundamental eigenmodes $\text{HE}_{\pm 11}$ are located around 5 GHz and the upper modes are around 10.5 GHz. In this configuration, the HE_{-21} mode appears first and therefore before the HE_{+21} mode.

The design of this resonator is not enough to obtain a circulation function, because in this case, the modes are not coupled. To couple the counter-rotating modes, the analytical methods are available for central conductors of disk type [10], [25] and for complex conductors such as WYE with stubs [24]. However, these coupling methods only deal with fundamental modes to achieve single-band circulators. Here, the objective is to obtain a dual-band operation by coupling fundamental and upper modes simultaneously, so these methods cannot be used. Therefore, a numerical method is used with the EM simulation software CST MWS. Striplines are added outside the ferrite resonator to complete the three symmetrical lines of the junction (Fig. 12).

The width S of these outer striplines adjusts the coupling of modes. To determine the width of the stripline allowing the ideal coupling of the fundamental and upper modes simultaneously, a parametric study is performed and presented in Fig. 13.

The stripline width that allows the simultaneous coupling of the first and the second bands with 20 dB of return loss (RL) is $S = 4$ mm. With the height of the stripline fixed by the height of resonators, the 4-mm-wide line has a characteristic impedance of 50 Ω. Therefore, it is not necessary to add a transformer on this circulator and a 50-Ω SMA connector can be directly integrated and soldered to this line.

At this stage of the study, the dc magnetic field inside the ferrite disks (Hi) has always been considered as homogeneous, uniform, and equal to 51 kA/m. In the reality, the dc magnetic field is obtained by permanent magnets on each side of these disks and the field emitted by these magnets is not uniform and is affected by edge effects. These effects have an impact on the dc magnetic field inside the ferrite disks' value, which will not be the same throughout the ferrite. Therefore, a magnetostatic (MS) study is carried out to dimension the magnets which will allow an internal field Hi, as stable as possible in the ferrite and as close as possible to the value determined during the

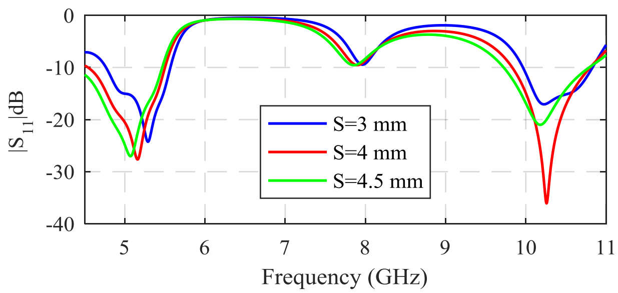

Fig. 13. EM simulations of Fig. 12 model with Fig. 11 central conductor and for different linewidths.

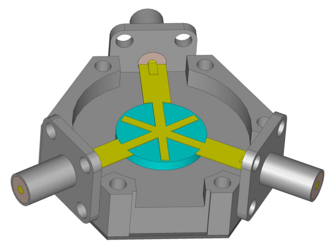

Fig. 14. Complete design of the unidirectional dual-band ferrite circulator.

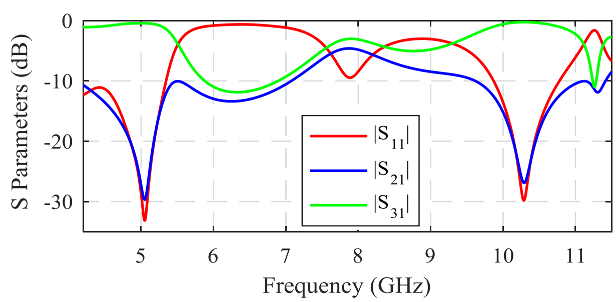

Fig. 15. MS-EM co-simulation S-parameters.

resonator dimensioning (Hi = 51 kA/m). MS simulations are performed using the CST MS solver. This design step consists of choosing the appropriate properties and sizes of permanent magnets using an iterative procedure. This procedure aims to achieve an internal field Hi as close as possible to 51 kA/m and as stable as possible in all ferrites. At each iteration, Hi is plotted in several ferrite planes. If the conditions of uniformity are not fulfilled, another iteration is performed with different radius and thickness until a correct result is obtained.

Finally, an electromagnetic/magnetostatic (MS-EM) co-simulation considering this real dc magnetic field generated by magnets is performed to model the complete design of the circulator, that is, including connectors, soldering, and so on (see Fig. 14).

The MS-EM co-simulation S-parameters' results are presented in Fig. 15.

As expected, the simulation results show a unidirectional circulation phenomenon around 5 and 10.3 GHz with a good isolation (Iso) and low insertion losses.

To validate these results, a prototype of this circulator is realized as shown in Fig. 16.

The structure is biased by two ferrite strontium magnets with 4300 G of remanent field. The measured S-parameters are presented in Fig. 17 and compared with those simulated with a

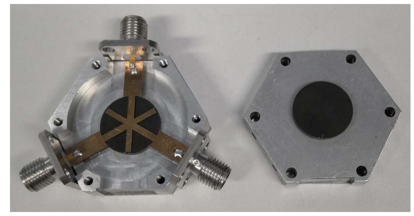

Fig. 16. Prototype of the unidirectional circulator.

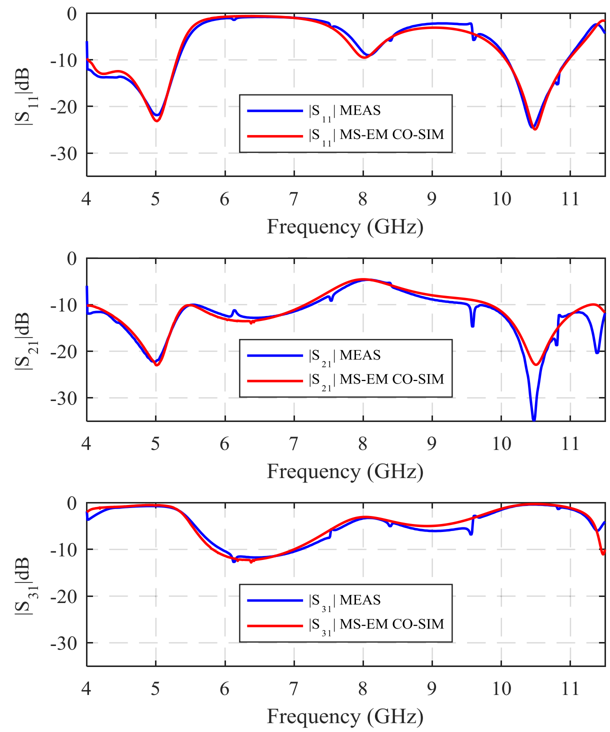

Fig. 17. Unidirectional dual-band ferrite circulator with weak bias field: MS-EM co-simulation and measurement.

relative permittivity of 13.4 instead of 14, which corresponds to an error of 4.3%. This error is consistent with the 5% accuracy given above.

The measurement results are close to the simulation and exhibit a unidirectional circulation direction. The RL and Iso are better than 20 dB on the [4.9–5.1 GHz] and [10.3–10.6 GHz] frequency bands with insertion losses lower than 0.78 and 0.45 dB, respectively.

For some specific applications, the required Iso is only 15 dB. With such requirements, the two BWs are better than 600 MHz.

Retro-simulations were carried out and it was shown that the spurious peaks in the measurements came from a minor shift in the alignment of the two ferrite disks.

Table II summarizes these performances and compares them with the measurement results in strong field of a unidirectional circulator presented in [7]. BWs are given for an Iso and RLs greater than 15 and 20 dB, respectively.

Table II shows that the objective of increasing the working frequency BW for a dual-band circulator is achieved because BWs have been almost doubled compared with previous studies presented in the literature. However, the comparison with

TABLE II
MEASUREMENT RESULTS' COMPARISON OF THE UNIDIRECTIONAL DUAL-BAND CIRCULATOR WITH THE LITERATURE

Circulator	**Weak field (this work)**		**Strong field** [7]		[26]	[26]	[27]	[28]	[29]
Type	**Stripline & Bi-band**		**Stripline & Bi-band**		**Stripline Mono-band**				
Central frequency	5.0 GHz	10.5 GHz	2.55 GHz	4.40 GHz	4.60 GHz	10.1 GHz	3.8 GHz	12 GHz	7.5 GHz
BW(%) for Iso > 15dB and RL > 15dB	13.5	5.9	5.8	1.1	NA	NA	NA	NA	>80
BW(%) for Iso > 20dB and RL > 20dB	4.0	2.9	2.2	0.5	8.7	9.9	26	25	NA

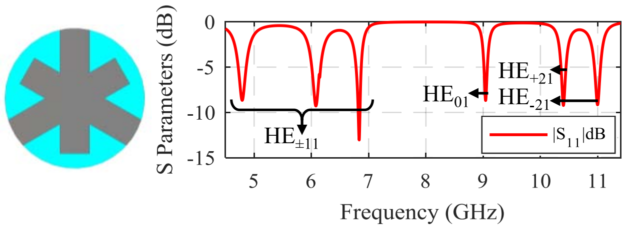

Fig. 18. Central conductor WYE with stubs with $W = 2.8$ mm and EM simulations of uncoupled ferrite resonator.

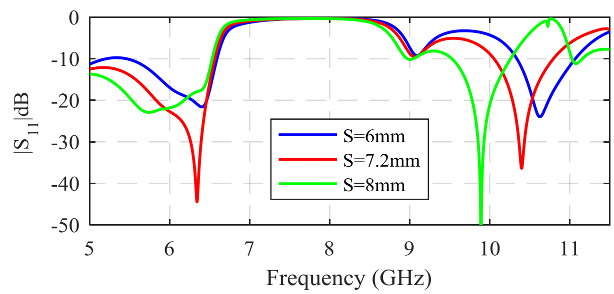

Fig. 19. $|S_{11}|$ parameters for different stripline widths.

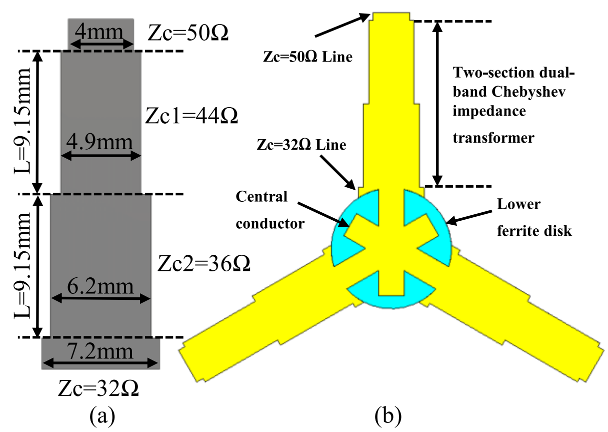

Fig. 20. (a) Numerical model of two-section dual-band Chebyshev impedance transformer and (b) coupled resonator with matching step.

the single-band stripline circulators [26]–[29] shows that better BWs can be reached if only one frequency band is targeted.

B. Bidirectional Dual-Band Circulator

In this paragraph, the design of a second dual-band circulator is presented. Section II showed that the order of appearance of the HE$_{\pm 21}$ modes can be inverted by changing the width of the WYE central conductor, which will lead to the inversion of the circulation direction on the second frequency band. Therefore, the ferrite disks used are the same as for the previous circulator design with the same dc magnetic field inside the ferrite disks' Hi of 51 kA/m. The only change with the previous circulator is the width of the central conductor, because it is now equal to 2.8 mm.

As for the previous paragraph, the eigenmodes' frequencies are obtained with the $|S_{11}|$-parameter of the weakly excited WYE resonator with linewidth of 2.8 mm (Fig. 18).

The resonance frequencies of eigenmodes are around an average of 6 GHz for the fundamental modes and around 10.5 GHz for the upper modes HE$_{\pm 21}$. The expected circulation frequencies of the circulator after coupling are therefore around 6 and 10.5 GHz.

As for the previous case, it is necessary to simultaneously couple the fundamental and the upper modes for exhibiting a circulation phenomenon on the two frequency bands. In this objective, the width of the feeding stripline has to be dimensioned. Fig. 19 presents the RL for different stripline widths S.

A circulation phenomenon appears simultaneously on the two frequency bands with good performances when $S = 7.2$ mm.

This line with such dimensions has a characteristic impedance of 32 Ω. As this impedance differs from 50 Ω, a matching circuit must be used to connect the circulator device to 50-Ω SMA connectors.

The matching circuit needs to convert an impedance of 32 to 50 Ω on two frequency bands. A dual-band matching method presented in [30] is used and consists of two sections of $\lambda/4$ lines. The wavelength is calculated using the average frequency between 6.1 and 10.5 GHz, that is, 8.3 GHz. This leads to adding two lines of 9.15-mm long with characteristic impedances of 36 and 44 Ω which allow an impedance matching from 32 to 50 Ω at 6.1 and 10.5 GHz.

The matching circuit [Fig. 20(a)] has been simulated using CST and shows that it involves losses of 0.007 dB at 6.1 GHz and 0.009 dB at 10.5 GHz. These losses are very small and not significant compared with circulator losses.

This transformer is then integrated to the circulator structure, as presented in Fig. 20(b).

The circulator is now adapted to 50 Ω and the connectors can be added. The next design step is the same as in Section III-A and consists of the MS-EM co-simulation. The magnets are the same as previously used since ferrites and dc magnetic field inside the ferrite disks are the same. The final design and the realized prototype are presented in Fig. 21.

TABLE III
MEASUREMENT RESULTS' COMPARISON OF THE BIDIRECTIONAL DUAL-BAND CIRCULATOR WITH THE LITERATURE

Circulator	**Weak field (this work)**		**Strong field** [7]		[26]	[26]	[27]	[28]	[29]
Type	**Stripline & Bi-band**		**Stripline & Bi-band**		**Stripline Mono-band**				
Central frequency	5.9 GHz	10.7 GHz	2.55 GHz	4.40 GHz	6.15 GHz	10.1 GHz	3.8 GHz	12 GHz	7.5 GHz
BW(%) for Iso > 15dB and RL > 15dB	19.2	3.4	5.0	1.5	NA	NA	NA	NA	>80
BW(%) for Iso > 20dB and RL > 20dB	13.6	1.9	2.2	0.7	8.1	9.9	26	25	NA

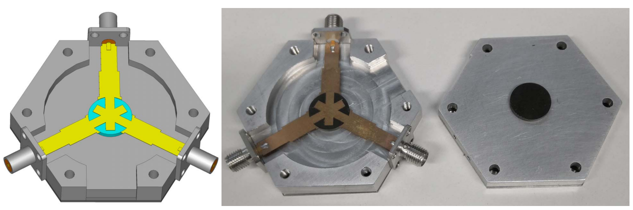

Fig. 21. Bidirectional dual-band ferrite circulator with weak bias field: complete numerical model after MS-EM co-simulation and prototype.

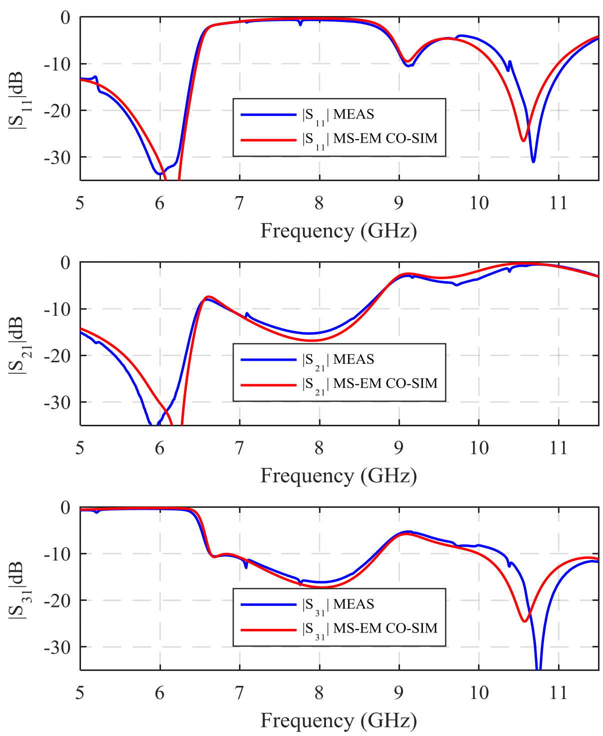

Fig. 22. Bidirectional dual-band ferrite circulator with weak bias field: MS-EM co-simulation and measurement.

As with the unidirectional case, the simulation is done with a relative permittivity of 13.4 instead of 14. As expected, the measured and simulated results exhibit a bidirectional circulation direction (Fig. 22).

The RL and Iso are better than 20 dB on the [5.5–6.3 GHz] and [10.6–10.8 GHz] frequency bands with insertion losses lower than 0.65 and 0.75 dB, respectively. With an Iso requirement of 15 dB, the BWs are larger than 1.1 GHz for the first band and 360 MHz for the second band.

Table III summarizes these performances and compares them with the measurement results in strong field of a bidirectional circulator presented in [7].

Similar to the unidirectional circulator, Table III shows that the objective of increasing the working frequency BW is met with a real improvement on the first frequency band. Moreover, when comparing BWs with the commercial stripline circulators [26], the first BW is better than the one of a single-band circulator operating at the same frequency. The second band is still narrower than the commercial standards. These narrower BWs result from the challenge of simultaneously coupled fundamental and upper modes.

IV. CONCLUSION

In this article, the first demonstration of a dual-band circulator operating on the weak field conditions has been presented. The frequency gap between the two operating bands has been chosen and is perfectly mastered. This has been possible, thanks to the development of a reliable methodology based on an eigenmodes analysis, which takes into account the influence of the shape and dimensions of the central conductor and the intrinsic ferrite properties. The parameters that affect the frequency ratio between counter-rotating modes and between the fundamental and upper modes have been identified, thanks to modal analyses. Indeed, these eigenmode analyses are at the basis of our methodology since they allow, according to the frequency specifications given by one or more applications, to determine the properties of ferrite resonators (4πMs, Hi,…) and the shapes of the central conductors. In addition to providing operating frequencies, these modal analyses can also predetermine the direction of circulation. Indeed, we have shown that by simply changing the central conductor, the upper modes' order can be reversed, leading to the change in the circulation direction. Finally, the measurement results have been compared with the ones presented in the literature and exhibit that working in the weak field area allows a great improvement of working BWs.

ACKNOWLEDGMENT

This work has been done in the framework of a joint laboratory INOGYRO (http://inogyro.xlim.fr) gathering the XLIM Research Institute, Limoges, France, and Inoveos SME, Brive-la-Gaillarde, France.

REFERENCES

[1] N. Hansen, S. Radzijewski, J.-P. Mohncke, and A. F. Jacob, "A low cost dual-band transmit-receive module for a commercial maritime radar with digital beamforming," in *Proc. 22nd Int. Microw. Radar Conf. (MIKON)*, Poznan, Poland, May 2018, pp. 527–530, doi: 10.23919/MIKON.2018.8405276.

[2] G. Macchiarella and S. Tamiazzo, "Design techniques for dual-passband filters," *IEEE Trans. Microw. Theory Techn.*, vol. 53, no. 11, pp. 3265–3271, Nov. 2005, doi: 10.1109/TMTT.2005.855749.
[3] S. Sun and L. Zhu, "Compact dual-band microstrip bandpass filter without external feeds," *IEEE Microw. Wireless Compon. Lett.*, vol. 15, no. 10, pp. 644–646, Oct. 2005, doi: 10.1109/LMWC.2005.856687.
[4] C.-M. Su and K.-L. Wong, "A dual-band GPS microstrip antenna," *Microw. Opt. Technol. Lett.*, vol. 33, no. 4, pp. 238–240, May 2002, doi: 10.1002/mop.10285.
[5] C.-X. Mao, S. Gao, Y. Wang, Q.-X. Chu, and X.-X. Yang, "Dual-band circularly polarized shared-aperture array for C-/X-band satellite communications," *IEEE Trans. Antennas Propag.*, vol. 65, no. 10, pp. 5171–5178, Oct. 2017, doi: 10.1109/TAP.2017.2740981.
[6] D. Q. Liu, M. Zhang, H. J. Luo, H. L. Wen, and J. Wang, "Dual-band platform-free PIFA for 5G MIMO application of mobile devices," *IEEE Trans. Antennas Propag.*, vol. 66, no. 11, pp. 6328–6333, Nov. 2018, doi: 10.1109/TAP.2018.2863109.
[7] H. Turki, L. Huitema, T. Monediere, B. Lenoir, and C. Breuil, "New concept validation of low-loss dual-band stripline circulator," *IEEE Trans. Microw. Theory Techn.*, vol. 67, no. 3, pp. 845–850, Mar. 2019, doi: 10.1109/TMTT.2018.2890632.
[8] H. Razavipour, G. Askari, F. Fesharaki, and H. Mirmohammad-Sadeghi, "A new high-power, dual-band, E-plane, ferrite circulator," in *Proc. IEEE EUROCON*, St. Petersburg, Russia, May 2009, pp. 20–25, doi: 10.1109/EURCON.2009.5167598.
[9] T. Mróz, J. Michałowski, R. Frender, and M. Zebrowski, "Dual—Band waveguide circulator for C and X bands," in *Proc. MIKON*, May 2008, pp. 1–4.
[10] H. Bosma, "On stripline Y-circulation at UHF," *IEEE Trans. Microw. Theory Techn.*, vol. MTT-12, no. 1, pp. 61–72, Jan. 1964, doi: 10.1109/TMTT.1964.1125753.
[11] C. E. Fay and R. L. Comstock, "Operation of the ferrite junction circulator," *IEEE Trans. Microw. Theory Techn.*, vol. 13, no. 1, pp. 15–27, Jan. 1965, doi: 10.1109/TMTT.1965.1125923.
[12] Y. S. Wu and F. J. Rosenbaum, "Wideband operation of microstrip circulators," in *Proc. IEEE G-MTT Int. Microw. Symp.*, Boulder, CO, USA, Jun. 1973, pp. 92–94, doi: 10.1109/GMTT.1973.1123103.
[13] M. Latrach, T. Monediere, and F. Jecko, "A new design of cylindrical closed triplate ferrite resonators compared with magnetic wall approximation," *IEEE Trans. Magn.*, vol. 26, no. 5, pp. 2856–2862, Sep. 1990, doi: 10.1109/20.104897.
[14] V. Laur *et al.*, "Self-biased Y-Junction circulators using Lanthanum-and cobalt-substituted strontium hexaferrites," *IEEE Trans. Microw. Theory Techn.*, vol. 63, no. 12, pp. 4376–4381, Dec. 2015, doi: 10.1109/TMTT.2015.2495218.
[15] A. Ashley, L. F. Marzall, Z. Popovic, and D. Psychogiou, "Frequency selective ferrite circulators with quasi-elliptic transmission response," in *Proc. 48th Eur. Microw. Conf. (EuMC)*, Madrid, Spain, Sep. 2018, pp. 211–214, doi: 10.23919/EuMC.2018.8541616.
[16] J. B. Davies and P. Cohen, "Theoretical design of symmetrical junction stripline circulators," *IEEE Trans. Microw. Theory Techn.*, vol. MTT-11, no. 6, pp. 506–512, Nov. 1963, doi: 10.1109/TMTT.1963.1125717.
[17] G. P. Riblet, "The extent of the similarity between below resonance and above resonance operation of standard circulator junctions," in *IEEE MTT-S Int. Microw. Symp. Dig.*, vol. 78, Jun. 1978, pp. 323–325, doi: 10.1109/MWSYM.1978.1123878.
[18] J. J. Green and F. Sandy, "Microwave characterization of partially magnetized ferrites," *IEEE Trans. Microw. Theory Techn.*, vol. 22, no. 6, pp. 641–645, Jun. 1974, doi: 10.1109/TMTT.1974.1128306.
[19] D. Polder, "Ferrite materials," *Proc. IEE–II, Power Eng.*, vol. 97, no. 56, pp. 246–256, Apr. 1950, doi: 10.1049/pi-2.1950.0076.
[20] P. Gelin, "New consistent model for ferrite permeability tensor with arbitrary magnetization state," *IEEE Trans. Microw. Theory Techn.*, vol. 45, no. 8, pp. 1185–1192, Aug. 1997, doi: 10.1109/22.618406.
[21] H. Bosma, "On the principle of stripline circulation," *Proc. IEE–B, Electron. Commun. Eng.*, vol. 109, no. 21S, pp. 137–146, Jan. 1962.
[22] J. Helszajn, *Stripline Circulator: Theory and Practice*. Hoboken, NJ, USA: Wiley, 2008, p. 614.
[23] J. W. Simon, "Broadband strip-transmission line Y-Junction circulators," *IEEE Trans. Microw. Theory Techn.*, vol. 13, no. 3, pp. 335–345, May 1965, doi: 10.1109/TMTT.1965.1125998.
[24] J. Helszajn and W. T. Nisbet, "Circulators using planar WYE resonators," *IEEE Trans. Microw. Theory Techn.*, vol. 29, no. 7, pp. 689–699, Jul. 1981, doi: 10.1109/TMTT.1981.1130430.
[25] S. I. Shams, M. Elsaadany, and A. A. Kishk, "Including stripline modes in the Y-Junction circulators: Revisiting fundamentals and key design equations," *IEEE Trans. Microw. Theory Techn.*, vol. 67, no. 1, pp. 94–107, Jan. 2019, doi: 10.1109/TMTT.2018.2880755.
[26] *Bx30xx Cobham Coaxial Circulators*. Accessed: May 12, 2019. [Online]. Available: https://www.cobham.com/communications-and-connectivity/electrical-and-electronic-equipment/microwave-components-and-systems/microwave-isolators-and-circulators/coaxial-product/docview/
[27] N. Jaiswal and P. Pradeepkumar, "Ultra-broadband C-band stripline co-axial isolator design," in *Proc. IEEE Indian Conf. Antennas Propogation (InCAP)*, Hyderabad, India, Dec. 2018, pp. 1–4, doi: 10.1109/INCAP.2018.8770783.
[28] A. Ghadiya, K. Trivedi, S. Soni, and P. Bhatt, "Wide band stripline circulator at ku band for space applications," in *IEEE MTT-S Int. Microw. Symp. Dig.*, Kolkata, India, Nov. 2018, pp. 1–4, doi: 10.1109/IMaRC.2018.8877303.
[29] H. Turki, L. Huitema, T. Monediere, B. Lenoir, and C. Breuil, "Complete methodology of low-loss ultra-wideband junction circulator," in *IEEE MTT-S Int. Microw. Symp. Dig.*, Philadelphia, PA, USA, Jun. 2018, pp. 746–749, doi: 10.1109/MWSYM.2018.8439670.
[30] S. J. Orfanidis, "A two-section dual-band Chebyshev impedance transformer," *IEEE Microw. Wireless Compon. Lett.*, vol. 13, no. 9, pp. 382–384, Sep. 2003, doi: 10.1109/LMWC.2003.817135.

Vincent Olivier was born in Bergerac, France, in 1996. He received the M.S. degree in telecommunications high frequencies and optics from Limoges University, Limoges, France, in 2018, where he is currently pursuing the Ph.D. degree at the XLIM Research Institute, in collaboration with the Inoveos, Brive-la-Gaillarde, France.

His main research interests include gyromagnetic devices as ferrite circulators or isolators and multiband passive devices.

Laure Huitema (Member, IEEE) received the M.S. and Ph.D. degrees in telecommunications high frequencies and optics from Limoges University, Limoges, France, in 2008 and 2011, respectively.

From 2011 to 2012, she was a Post-Doctoral Research Fellow with the Atomic Energy Commission (CEA), Laboratory of Electronics and Information Technology (LETI), Grenoble, France. She is currently an Associate Professor with the Antennas and Signals Team within the RF systems' axis of the XLIM Research Institute, Limoges University. She is currently the Director of the joint laboratory INOGYRO, XLIM Research Institute, which brings together the XLIM Laboratory, Limoges, and Inoveos, Brive-la-Gaillarde, France. Her research interests include reconfigurable antennas, dielectric resonator antennas, miniature antennas, multiband antennas, and circulators. More recently, she has been working on new components for their integration inside antennas. In this framework, she is the Project Leader of a H2020 European Project called MASTERS.

Dr. Huitema was a recipient of the Best Student Paper Award at the 2010 IEEE International Workshop on Antenna Technology and the Best Student Paper Award at the 2010 JCMM Conference. In 2020, she won the bronze medal of the CNRS (the French National Centre for Scientific Research).

Bertrand Lenoir was born in 1974. He received the Ph.D. degree from the University of Limoges, Limoges, France, in 2001.

He is currently the Chief Technology Officer (CTO) of Inoveos, Brive-la-Gaillarde, France. His main research interests include design and optimization of isolators, circulators, filters, couplers, and passive or active subsystems.

Hamza Turki was born in Bizerta, Tunisia, in 1991. He received the M.S. and Ph.D. degrees in telecommunications, high frequencies and optics from Limoges University, Limoges, France, in 2015 and 2018, respectively.

He is currently a Research and Development Engineer with Inoveos, Brive-la-Gaillarde, France. His main research interests include gyromagnetic devices, passive filters/diplexers, couplers, and antennas.

Dr. Turki received the Best Student Paper Award at the 2018 National Conference on Material and Microwave Characterization.

Christophe Breuil was born in Brive-la-Gaillarde, France, in 1970.

He is currently a Design Manager of Inoveos, Brive-la-Gaillarde, where he is in charge of mechanical studies and manufacturing of isolators, circulators, couplers, and microwave filters. He also contributes significantly to tests and measurements of these products.

Philippe Pouliguen (Member, IEEE) received the M.S. degree in signal processing and telecommunications, the Doctoral degree in electronic, and the Habilitation à Diriger des Recherches degree from the University of Rennes 1, Rennes, France, in 1986, 1990, and 2000, respectively.

In 1990, he joined the Direction Générale de l'Armement (DGA), DGA Information Superiority (DGA/IS), Bruz, France, where he was a Senior Expert in electromagnetic radiation and radar signatures. He was also in charge of the Expertise and ElectoMagnetism Computation (EMC) Laboratory, DGA/IS. From 2009 to 2018, he was the Head of acoustic and radio-electric waves scientific domain at DGA, Paris, France. Since 2018, he has been the Innovation Manager of the acoustic and radio-electric waves domain with Agence Innovation Défense (AID), Paris. His research interests include electromagnetic scattering and diffraction, radar cross-section (RCS) measurement and modeling, asymptotic high-frequency methods, radar signal processing and analysis, antenna scattering problems, and electronic bandgap materials.

Thierry Monediere was born in Tulle, France, in 1964. He received the Ph.D. degree from the IRCOM Laboratory, University of Limoges, Limoges, France, in January 1990.

He is currently a Professor with the Antennas and Signals Team, XLIM Research Laboratory, University of Limoges. He develops his research activities in this laboratory and works on multifunction antennas, miniature antennas, antenna arrays, and active antennas. He also studies gyromagnetic devices as ferrite circulators or isolators.